Cambridge Centre for Computational Chemical Engineering

University of Cambridge

Department of Chemical Engineering

Preprint ISSN 1473 – 4273

First-principles thermochemistry for the combustion of a $TiCl_4$ and $AlCl_3$ mix.

Raphael Shirley [1] Yaoyao Liu [1] Tim Totton [1] Richard H. West [1] Markus Kraft [1]

released: November 5, 2009

[1] Department of Chemical Engineering and Biotechnology
University of Cambridge
New Museums Site
Pembroke Street
Cambridge, CB2 3RA
UK
E-mail: mk306@cam.ac.uk

Preprint No. 74

c4e

Key words and phrases: titanium dioxide, thermochemistry, density functional theory, $AlCl_3$, $TiCl_4$

Edited by
Cambridge Centre for Computational Chemical Engineering
Department of Chemical Engineering
University of Cambridge
Cambridge CB2 3RA
United Kingdom.

Fax: + 44 (0)1223 334796
E-Mail: c4e@cheng.cam.ac.uk
World Wide Web: http://www.cheng.cam.ac.uk/c4e/

Abstract

$AlCl_3$ is added in small quantities to $TiCl_4$ fed to industrial reactors during the combustion synthesis of titanium dioxide nanoparticles in order to promote the rutile crystal phase. Despite the importance of this process a detailed mechanism including $AlCl_3$ is still not available. This work presents the thermochemistry of many of the intermediates in the early stages of the mechanism, computed using quantum chemistry. The enthalpies of formation and thermochemical data for AlCl, AlO, AlOCl, $AlOCl_2$, AlO_2, AlO_2Cl, $AlOCl_3$, AlO_2Cl_2, AlO_3ClTi, AlO_2Cl_2Ti, AlO_2Cl_4Ti, $AlOCl_5Ti$, AlO_2Cl_3Tia, AlO_2Cl_2Ti, AlO_2Cl_5Ti, $AlOCl_4Ti$, AlO_2Cl_3Tib, $AlCl_7Ti$, $AlCl_6Ti$, Al_2Cl_6, Al_2O_2Cl, $Al_2O_2Cl_3$, $Al_2O_3Cl_2$, $Al_2O_2Cl_2$, Al_2OCl_4, Al_2O_3, and Al_2OCl_3 were calculated using density functional theory (DFT). A full comparison between a number of *ab initio* methods is made for one of the important species, AlOCl, in order to validate the use of DFT and gauge the magnitude of errors involved with this method. Finally, equilibrium calculations are performed to try to identify which intermediates are likely to be most prevalent in the high temperature industrial process, and as a first attempt to characterize the nucleation process.

Contents

1 Introduction

Titanium dioxide (TiO_2) is widely used as a pigment, as a catalyst support, and as a photocatalyst. The combustion of titanium tetrachloride ($TiCl_4$) to synthesize TiO_2 nanoparticles is a multi-million tonne per year industrial process [8]. In this "chloride" process, purified titanium tetrachloride is oxidized at high temperatures (1500–2000 K) in a pure oxygen plasma or flame to produce TiO_2 particles [6, 10]. The overall stoichiometry of this oxidation process is

$$TiCl_{4\,(g)} + O_{2\,(g)} \rightarrow TiO_{2\,(\text{rutile nanoparticles})} + 2\,Cl_{2\,(g)}. \tag{1}$$

TiO_2 crystallizes in three different forms: rutile, anatase and brookite. $AlCl_3$ is often added to industrial reactors in order to promote formation of the rutile phase. The rutile phase is photochemically stable with a high refractive index compared to anatase and therefore preferred for pigmentary applications. $AlCl_3$ is added in small quantities ($<$ 5%mol) and it is unclear how significantly it alters the early gas phase reactions.

Although the chloride process is a mature technology, which has been used in industry since 1958, understanding of the gas-phase reactions of $TiCl_4$ remains incomplete[16]. Recently, West *et al.* have developed a detailed kinetic model for the process including thermochemical data for the titanium oxychloride species involved[29–31]. However, these models do not attempt to include the impact of $AlCl_3$ on the reaction kinetics or on the properties of the particles formed. The paper by Akhtar *et al.* describes how $AlCl_3$ influences the crystal phase[2] of the particles but does not offer a mechanism to explain how. Some authors suggest that Al accelerates the anatase to rutile transformation[18, 22] but this is hard to reconcile with the theoretical studies showing that there is no significant thermodynamic bias between the doped phases[15, 24, 27]. It may be that Al lowers the barrier to phase transformation but it is also possible that in the industrial reactors, the phase is determined by the nucleation process. A small number of $TiAlCl_x$ species have been studied experimentally[14, 25] but the system with excess oxygen has not been investigated. Varga *et al.*[28] provide thermochemical data for some of the aluminium oxyhalides from computational studies but a number of possible species, particularly dimers, are missing. It is also possible that the impact of $AlCl_3$ is entirely physical in which case it would be useful to rule out any significant chemical interaction.

The aim of this work is to provide thermochemical data for important titanium/aluminium oxychloride species ($Al_iO_jCl_kTi_l$), which will enable the development of detailed kinetic models of the combustion of titanium tetrachloride with aluminium trichloride. The results from three DFT functionals are compared, giving some indication of the reliability of DFT for these transition metal oxychloride species.

Since the optical properties of TiO_2 depend strongly on particle size, a major technological issue in this large scale industrial process is precisely controlling the particle size distribution. The size distribution is expected to depend strongly on the particle nucleation rate, which in turn may depend strongly on the concentration of $AlCl_3$. We have used the new thermochemical data to perform equilibrium calculations to identify which intermediates are likely to be most prevalent in the high temperature industrial process. This is a first step towards understanding how $AlCl_3$ effects the nucleation process and how it determines crystal phase.

2 Computational Method

2.1 Species Generation

As no reaction scheme currently exists for the gas phase reactions of $AlCl_3$, it was necessary to propose possible intermediate aluminium species that may by created by the reactions. These were then subject to geometry optimization calculations using density functional theory.

A script written in the Perl programming language was used to automatically generate possible aluminium species from those titanium species proposed by West *et al.*[31] in their mechanism for combustion synthesis of TiO_2. However, this is not as simple as a direct substitution of Al atoms for Ti atoms in each structure. There are two sources of additional complexity:

1. Some species have more than one Ti atom. Thus, aluminium-containing species may be generated with some or all Ti atoms substituted for Al atoms.
2. Valence differs between titanium (+4) and aluminium (+3) atoms. As such, species generated by direct substitution of Al for Ti are often unfeasible, and different aluminium-containing species may also be generated by removing one or more directly bonded atoms.

Thus, the Perl script uses conditional loops to systematically include possible permutations arising from (1) and (2) and exclude clearly unfeasible aluminium species (e.g., five directly-bonded atoms). Figure 1 illustrates the possible aluminium-containing species generated (within reason) from $Ti_2O_2Cl_4$.

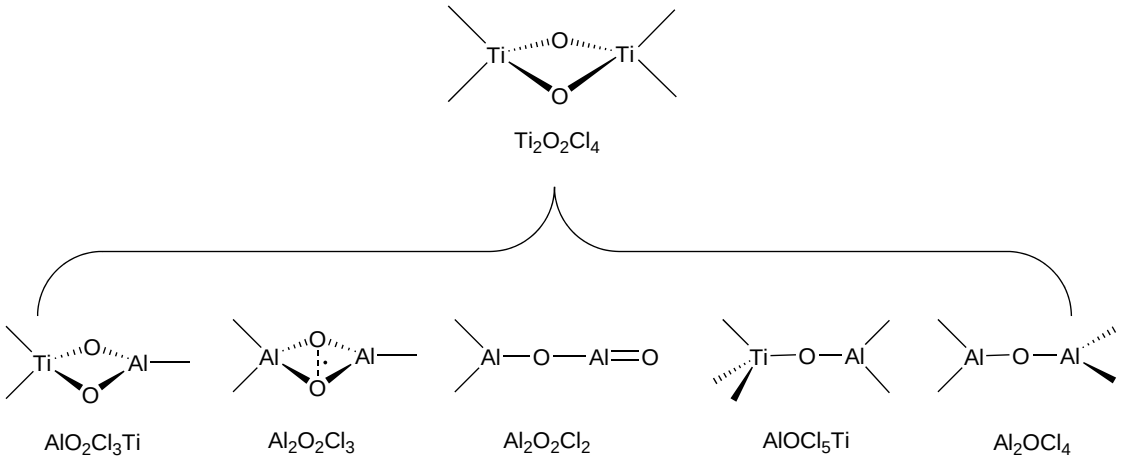

Figure 1: *Generating possible aluminium-containing species from* $Ti_2O_2Cl_4$. *Unlabeled atoms are chlorine.*

Where appropriate, further species were added heuristically in addition to those automatically generated. Many of the generated structures could not be made to converge to a stable geometry under DFT geometry optimization and are excluded.

2.2 Quantum Chemistry Calculations

For consistency and comparability with the previous work of West *et al.*[29] on $Ti_xO_yCl_z$ species, most calculations in this work were performed with the same three functionals: B3LYP[3, 17, 26], B97-1[13], and mPWPW91[1, 21]. These were carried out using the Gaussian 03 package[9].

Table 1 compares basis sets and *ab initio* methods for the single species AlOCl. The basis sets of Pople *et al.* (row 1-5 Table 1) do not show systematic convergence of $\Delta_f H^\circ_{298.15\,K}$ with increasing basis set size. However, it is individual species' electronic energy that is directly affected by basis-set truncation error and Figure 2 shows inconsistent improvement in energies for each species used to calculate $\Delta_f H^\circ_{298.15\,K}$. Nonetheless, on average larger basis sets should yield better accuracy. The correlation-consistent basis sets do exhibit systematic improvement in the calculated formation enthalpies, which is expected by their design.

The accuracy of results from MPn methods, MP3 in particular, are erratic and possibly arise from sensitivity to spin contamination for the open-shell triplet ground state of O_2 (used to calculate $\Delta_f H^\circ_{298.15\,K}$, cf. Reaction 3).

The agreement between CCSD(T) and B3LYP for this geometry gives confidence to the DFT methods and reaction scheme employed in this work.

Table 1: *Calculated $\Delta_f H^\circ_{298.15\,K}$ values (kJ/mol) for AlOCl from different* ab initio *methods and basis sets using Reaction 3.*

	Hartree-Fock		*post Hartree-Fock*					*DFT*
Basis set	HF	PUHF	MP2	MP3	MP4	CCSD	CCSD(T)	B3LYP
3-21G	-102	-93	-247	-178	-311	-219	-244	-220
6-31G	-136	-125	-281	-221	-323	-256	-272	-243
6-311G	-131	-119	-278	-215	-316	-250	-266	-247
6-311G(d,p)	-81	-68	-194	-147	-212	-175	-191	-203
6-311+G(d,p)	-96	-82	-210	-139	-232	-189	-204	-216
cc-pVDZ	-83	-70	-191	-145	-218	-174	-190	-209
cc-pVTZ	-109	-94	-229	-181	-247	-204	-221	-234
aug-cc-pVTZ	-112	-97	-239	-190	-256	-211	-229	-236

Calculations consist of single point energies based on the B97-1/6-311+G(d,p)-optimized geometry, with thermal contributions to enthalpy calculated from B97-1/6-311+G(d,p) frequencies

2.3 Statistical Mechanics and Equilibrium Composition

Heat capacities (C_p°), thermal enthalpy ($H(T) - H(0\ K)$), and entropies (S) were calculated for temperatures in the range 100-4000 K using the rigid rotator harmonic oscillator (RRHO) approximation, taking unscaled vibrational frequencies and rotational constants from the B3LYP calculations. The contribution of the excited electronic states to the partition function is ignored.

Polynomials in the NASA[12] form were fitted to C_p° (T)/R, H° and S° over the temperature ranges 100-x K and x-4000 K, constrained to ensure that all three functions are

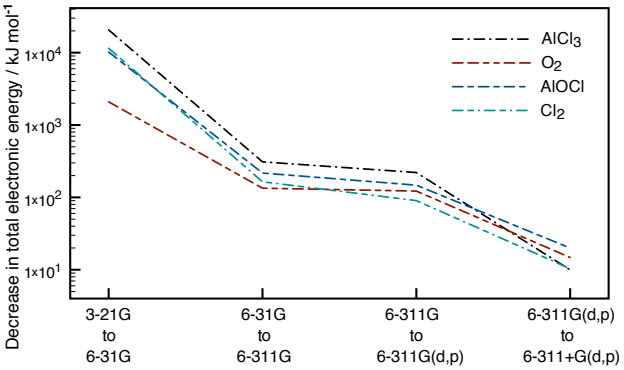

Figure 2: *Decrease in total electronic energy with larger basis sets (i.e., reduction in basis-set truncation error). Energies are calculated by the B3LYP functional.*

continuous and smooth across the boundary, x, which was varied to optimize the fit. Using these NASA polynomials, the equilibrium composition as a function of temperature was calculated using the open source software Cantera[11].

3 Results and Discussion

3.1 Geometries

A large number of the species generated automatically and some of the species generated manually could not be made to converge to a sensible structure under geometry optimization with the B3LYP functional. Where a given molecule had numerous isomers, the lowest energy isomer was chosen and all others were neglected. Other species were omitted because they had very large enthalpies of formation and were only present to a negligible degree at equilibrium. Figure 3 shows the geometries of all the convergent species after optimization at the B3LYP/6-311+G(d,p) level of theory. The gaussian output files and the geometries in mol format are available as supporting information.

3.2 Enthalpy of Formation

The paucity of literature thermochemical data for the aluminium oxychloride species investigated in this work means it was not feasible to form isodesmic or isogyric reactions linking a species with unknown $\Delta_f H^\circ_{298.15\,K}$ to species for which $\Delta_f H^\circ_{298.15\,K}$ have been experimentally determined. An obvious starting point for AlOCl, for instance, might have been the isogyric reaction (all three species are in singlet states)

$$\tfrac{1}{3}\mathrm{AlCl_3\,(g)} + \tfrac{1}{3}\mathrm{Al_2O_3\,(g)} \rightleftharpoons \mathrm{AlOCl\,(g)}. \qquad (2)$$

The NIST–JANAF thermochemical tables list $\Delta_f H^\circ_{298.15\,K} = -584.59$ kJ/mol for gaseous $\mathrm{AlCl_3}$ [4]. However, reliable thermochemical data for $\mathrm{Al_2O_3}$ are only available for the

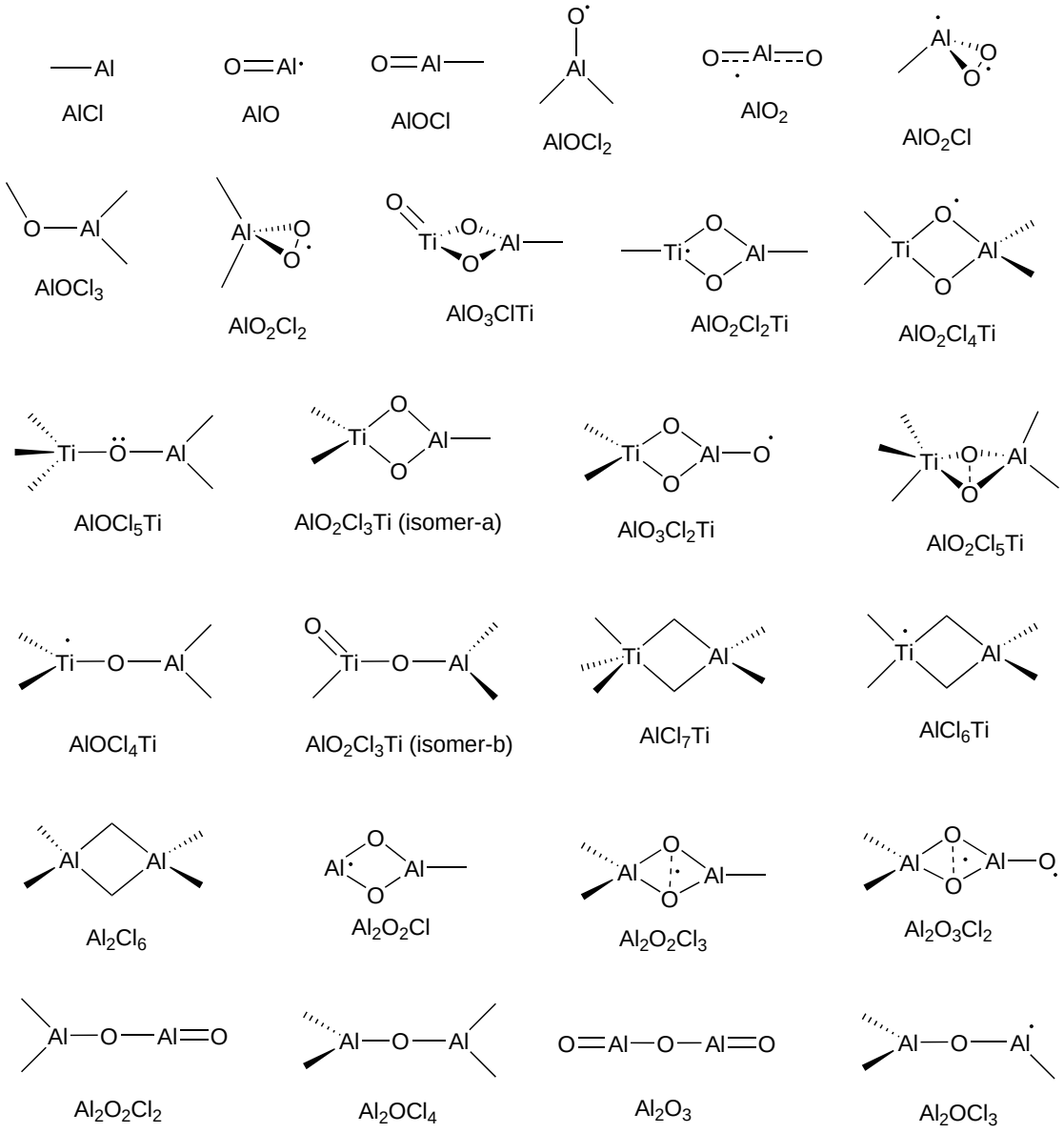

Figure 3: *Molecular geometries after optimization with B3LYP/6-311+G(d,p). Unmarked atoms are chlorine. Exact geometries are available in the supporting information.*

condensed phase; the gaseous species has only been observed in plasmas [7]. Hence Reaction Equation 2 could not be used to determine $\Delta_f H^\circ_{298.15\,K}$ for AlOCl.

The validity of the few available experimental data for $Al_xO_yCl_z$ species is also rather questionable. Varga *et al.* [28] suggest the JANAF value $\Delta_f H^\circ_{298.15\,K}$ = −348.11 kJ/mol for $AlOCl_{(g)}$ may require review; they cite a value of −280.3 kJ/mol from experiment. Table 2 also shows the considerable discrepancy between values reported in JANAF and the CRC Handbook [19] for less observable aluminium species.

Table 2: *Literature values of $\Delta_f H^\circ_{298.15\,K}$ (kJ/mol) for some aluminium species differ significantly.*

$\Delta_f H^\circ_{298.15\,K}$	CRC[19]	JANAF[4]
Al_2O	−130.0	−145.19
AlO	91.2	66.94
AlCl	−47.7	−51.46
$AlCl_2$	−331.0	−280.33
$AlCl_3$	−583.2	−584.59
$TiCl_4$	−763.2	−763.16

Given these constraints, the following reaction scheme was used to determine enthalpies of formation:

$$a\,\mathrm{AlCl_3\,(g)} + b\,\mathrm{TiCl_4\,(g)} + \tfrac{1}{2}c\,\mathrm{O_2\,(g)} \rightleftharpoons \mathrm{Al}_a\mathrm{O}_c\mathrm{Cl}_d\mathrm{Ti}_b\,\mathrm{(g)} + \tfrac{1}{2}(3a+4b-d)\,\mathrm{Cl_2\,(g)}. \quad (3)$$

This reaction is generally anisodesmic and often anisogyric; however, literature values of $\Delta_f H^\circ_{298.15\,K}$ for $AlCl_3$ and $TiCl_4$ are at least in good agreement with each other (Table 2). The main source of error in anisogyric reactions is due to systematic errors associated with given bonds where correlation energy is inaccurate at computationally realistic levels of theory [5]. However, these errors are in general likely to be smaller than or at least comparable to errors that might propagate through a series of coupled isodesmic/isogyric reactions with unreliable experimental $\Delta_f H^\circ_{298.15\,K}$ of the order of those seen in Table 2. If and when accurate experimental data becomes available enthalpies can be rapidly recalculated from the information available in the supporting information.

Calculated formation enthalpies are consolidated in Table 3 alongside the few literature values that exist. The right hand column shows the value that was used for the equilibrium calculations performed here. The enthalpy that is chosen for the equilibrium calculations is that calculated using B3LYP, or, if experimental data is available, that theoretical value that is closest to the mean of the experimental values. The absence of reliable experimental data makes validation of the $\Delta_f H^\circ_{298.15\,K}$ values somewhat difficult. However, where available the literature values agree reasonably well ($\pm\sim$40 kJ/mol). Agreement between the pure DFT (mPWPW91) and hybrid functionals (B3LYP, B97-1) is also good; these are calculated independently and thus their consistency gives confidence to the results. For example, the literature value of $\Delta_f H^\circ_{298.15\,K}$ = −1295 kJ/mol for Al_2Cl_6[4] agrees well with −1255, −1270, and −1274 kJ/mol calculated by B3LYP, B97-1, and mPWPW91, respectively; the spread between functionals is 19 kJ/mol in this case. Errors of this order

Table 3: *Calculated $\Delta_f H^{\circ}_{298.15\,K}$ values (kJ/mol) for three functionals with the 6-311+G(d,p) basis set using Reaction 3.*

	DFT calculation				*Literature*		
species	B3LYP	B97-1	mPWPW91	B3LYP[a]	JANAF[4]	CRC[19]/other	used
AlCl	−74	−57	−77	−85	−51	−47.7	−57
AlO	75	101	58	51	67	91.2	75
AlOCl	−216	−199	−230	−236	−348	−280.3[28]	−236
$AlOCl_2$	−412	−399	−396	−424			−412
AlO_2	−49		−72	−79	−86		−79
AlO_2Cl	−118	−101	−138	−145			−118
$AlOCl_3$	−514						−514
AlO_2Cl_2	−471	−468	−480	−494			−471
AlO_3ClTi	−957						−957
AlO_2Cl_2Ti	−936						−936
AlO_2Cl_4Ti	−1230						−1230
$AlOCl_5Ti$	−1107	−1091	−1058				−1107
AlO_2Cl_3Tia	−1229	−1214	−1223				−1214
AlO_3Cl_2Ti	−1044	−1017	−1021				−1017
AlO_2Cl_5Ti	−1291	−1326					−1326
$AlOCl_4Ti$	−1117						−1117
AlO_2Cl_3Tib	−1157						−1157
$AlCl_7Ti$	−1361						−1361
$AlCl_6Ti$	−1207						−1207
Al_2Cl_6	−1255	−1274	−1270		−1295		−1274
Al_2O_2Cl	−657						−657
$Al_2O_2Cl_3$	−1030	−1012	−1032				−1030
$Al_2O_3Cl_2$	−842						−842
$Al_2O_2Cl_2$	−815						−815
Al_2OCl_4	−1186						−1186
Al_2O_3	−441	−397					−441
Al_2OCl_3	−836						−836

Calculations consist of geometry optimisation and vibrational analysis with the specified functional. The final column indicates the values used for equilibrium calculations. [a]with the aug-cc-pVTZ basis set.

of magnitude are expected and consistent with those obtained by West *et al.* [29] for titanium oxychloride species. Reaction Equation 3 is still preferred over direct computation of $\Delta_f H^\circ_{298.15\,K}$ using atomization reactions; there is vastly more electronic correlation energy in molecules than in a collection of single atoms and retaining at least some bonds is always preferable *provided* the reference formation enthalpies taken from literature are reliable. West *et al.* [29] demonstrated a spread of 253 kJ/mol between formation enthalpies for TiO_2Cl_3 computed through atomisation (-865, -612 and -694 kJ/mol), which reduced to a spread of 38 kJ/mol when determined using an isogyric reaction.

3.3 Thermochemistry

Table 4 shows computed molecular and standard thermochemical data for species convergent under geometry optimization at the B3LYP/6-311+G(d,p) level of theory. Excited electron states are not considered. The smallest excitation energy was for $Al_2O_3Cl_2$ where the singlet state was found to be 130 kJ/mol higher than the triplet state and thus does not contribute significantly to the thermochemistry. This was also the only species to favor the higher spin state, which yields a C_{2v} conformation and higher symmetry order than the C_1 singlet-state structure. In other species, the lowest-energy states of different spin states from the ground state were typically several hundred kJ/mol higher in energy, and thus contribution of these to the molecular partition function will be insignificant. It is instructive to compare the entropy to the sparse literature values in order to reassure ourselves that the equilibrium plots are meaningful. Entropy makes a comparable contribution to the free energy at high temperatures and at very high temperatures (> 2000 K) dominates the free energy.

Table 5 shows that agreement for the entropy is stronger than for $\Delta_f H^\circ_{298.15\,K}$. This is probably because DFT produces reliable geometries and entropy is not directly affected by errors due to bond energies. It also goes some way to validating the RRHO assumption for this system and suggests that electronic contributions are not significant. Experimentally measured enthalpies of formation would be useful for improving thermochemistry. At the high temperatures of an industrial reactor enthalpy and entropy are of similar importance to the equilibrium concentration.

3.4 Equilibrium Composition

Computed equilibrium data are shown in Figure 4 for a mixture initially containing $AlCl_3$ and $TiCl_4$ at conditions similar to those of the industrial chloride process [2] using thermochemical data calculated by this work. In industrial reactors it is common to use quantities of $AlCl_3$ ranging from 0 to 10 %mol[23]. We first tested a number of low concentrations of $AlCl_3$ in order to gauge the sensitivity to initial concentration. In fact the behavior of the high concentration species is very *insensitive* to the amount of Al. We therefore chose a relatively large amount of $AlCl_3$ (5 %mol) in order to produce instructive graphs that highlight the impact of Al. Figure 4 incorporates the titanium species from the TiO_2 mechanism proposed by West *et al.*[31]. Thermochemical data for $TiCl_x$ ($x = 1, \ldots, 4$), TiO, TiO_2, chlorine oxides and standard gases were taken from the NASA database[20].

Table 4: *Standard thermochemistry at 298.15 K and molecular properties calculated at the B3LYP/6-311+G(d,p) level of theory for stable electronic ground states using Reaction 3. The electronic degeneracy, g, is included.*

species	g	$\Delta_f H^\circ_{298.15\,K}$ kJ/mol	$S^\circ_{298.15\,K}$ J/mol K	rot. const. GHz	vibrational frequencies cm^{-1}
AlCl	1	−74	228	7.0380	452
AlO	2	75	219	18.5982	925
AlOCl	1	−216	248	3.0948	178, 178, 485, 1108
$AlOCl_2$	2	−412	320	5.0340 2.1351 1.4992	143, 153, 213, 425, 624, 818
AlO_2	2	−49	236	5.7265	215, 215, 768, 826
AlO_2Cl	3	−118	313	14.388 2.5526 2.4810	143, 161, 411, 478, 605, 1144
$AlOCl_3$	1	−514	363	2.4067 1.1790 0.7913	77, 85, 137, 215, 218, 412, 609, 629, 906
AlO_2Cl_2	2	−471	340	2.8383 2.0287 1.2715	141, 155, 164, 198, 398, 461, 626, 675, 1135
AlO_3ClTi	1	−957	355	7.0330 0.8439 0.8017	78, 131, 181, 248, 312, 356, 559, 562, 707, 768, 847, 1038
AlO_2Cl_2Ti	2	−936	384	9.8416 0.5366 0.5088	29, 73, 115, 165, 257, 312, 420, 558, 578, 725, 767, 842
AlO_2Cl_4Ti	2	−1230	470	0.9708 0.4985 0.3581	34, 54, 84, 97, 108, 125, 170, 188, 276, 282, 399, 415, 448, 500, 554, 587, 685, 830
$AlOCl_5Ti$	3	−1107	534	0.7408 0.2748 0.2697	8, 28, 29, 60, 76, 97, 130, 141, 193, 243, 255, 284, 289, 369, 449, 585, 618, 996
AlO_2Cl_3Tia	1	−1157	464	1.4896 0.3705 0.3407	15, 28, 38, 71, 109, 153, 207, 259, 277, 332, 448, 591, 616, 994, 1071
AlO_3Cl_2Ti	2	−1044	401	1.7052 0.8143 0.6182	58, 106, 111, 164, 166, 177, 318, 332, 465, 505, 577, 683, 762, 768, 939
AlO_2Cl_5Ti	1	−1291	514	0.7465 0.3527 0.2843	27, 29, 56, 93, 101, 116, 129, 159, 185, 193, 241, 244, 280, 363, 382, 461, 471, 490, 601, 661, 755
$AlOCl_4Ti$	2	−1117	479	1.0230 0.3249 0.3177	10, 30, 32, 84, 95, 135, 148, 248, 257, 307, 404, 484, 587, 620, 994
AlO_2Cl_3Tib	1	−1229	406	1.7036 0.5327 0.4408	47, 97, 104, 148, 166, 174, 284, 326, 422, 504, 576, 590, 763, 767, 852
$AlCl_7Ti$	1	−1361	540	0.6225 0.2666 0.2536	13, 27, 74, 94, 101, 110, 123, 139, 160, 168, 168, 195, 216, 288, 335, 371, 433, 467, 492, 511, 596
$AlCl_6Ti$	2	−1207	503	0.7476 0.3465 0.2870	23, 48, 78, 83, 84, 106, 118, 154, 163, 194, 266, 291, 325, 376, 429, 491, 498, 602
Al_2Cl_6	1	−1255	473	0.7768 0.3902 0.3204	22, 63, 95, 116, 117, 129, 137, 165, 175, 217, 263, 311, 331, 412, 475, 514, 608, 617
Al_2O_2Cl	2	−657	322	9.7125 1.4497 1.2614	116, 151, 336, 352, 594, 628, 730, 762, 837
$Al_2O_2Cl_3$	2	−1030	416	1.8714 0.5182 0.4345	23, 110, 125, 139, 158, 201, 255, 280, 445, 446, 567, 586, 664, 714, 902
$Al_2O_3Cl_2$	3	−842	409	1.8678 0.7845 0.6072	27, 129, 130, 139, 173, 200, 263, 306, 437, 477, 588, 655, 694, 718, 972
$Al_2O_2Cl_2$	1	−815	384	2.2057 0.6983 0.5304	42, 71, 134, 174, 204, 287, 297, 349, 576, 620, 1000, 1209
Al_2OCl_4	1	−1186	445	1.1094 0.3538 0.3538	13, 39, 39, 110, 155, 179, 179, 280, 280, 323, 451, 612, 612, 669, 1113
Al_2O_3	1	−441	293	1.0077	71, 71, 186, 199, 312, 313, 420, 929, 1137, 1234
Al_2OCl_3	2	−836	425	1.8729 0.5101 0.4305	17, 47, 61, 134, 173, 237, 264, 362, 480, 605, 632, 1079

Table 5: *Comparison of $S^{\circ}_{298.15\ K}$ values (J/mol K) for three functionals with the 6-311+G(d,p) basis set.*

	DFT calculation				*Literature*		*Max. error*	
species	B3LYP	B97-1	mPWPW91	B3LYP[a]	JANAF[4]	CRC[19]/other	DFT	Lit.
$TiCl_4$	353.4	353.8	355.2		354.8	353.2	1.8	2.0
Cl_2	223.6	223.3	223.7	223.1	223.1	223.1	0.6	0.6
O_2	205.1	205.1	205.3	205.0	205.1	205.2	0.2	0.2
$AlCl_3$	313.9	313.9	314.9	314.0	314.4		1.0	0.4
AlCl	228.3	228.2	228.4	228.3	228.0	228.1	0.2	0.4
AlO	218.7	218.7	218.7	218.6	218.3	218.4	0.1	0.4
AlOCl	247.7	247.7	248.4	247.7	248.9		0.7	0.4
$AlOCl_2$	319.7	319.9	322.5	319.3			3.2	
AlO_2	236.3		236.4	236.5	251.8		0.3	15.3
AlO_2Cl	313.2	312.9	314.1	312.8			1.3	
$AlOCl_3$	362.7							
AlO_2Cl_2	340.0	345.8	347.5	345.3			7.5	
AlO_3ClTi	355.4							
AlO_2Cl_2Ti	384.3							
AlO_2Cl_4Ti	469.5							
$AlOCl_5Ti$	533.6	532.3	538.9				6.6	
AlO_2Cl_3Tia	405.8	406.0	409.1				3.2	
AlO_3Cl_2Ti	401.0	401.4	406.0				5.0	
AlO_2Cl_5Ti	513.6	508.4					5.1	
$AlOCl_4Ti$	478.6							
AlO_2Cl_3Tib	463.6							
$AlCl_7Ti$	539.9							
$AlCl_6Ti$	503.2							
Al_2Cl_6	473.2	473.7	476.7		475.0		3.5	1.8
Al_2O_2Cl	322.1							
$Al_2O_2Cl_3$	416.1	416.9	392.6				24.2	
$Al_2O_3Cl_2$	409.4							
$Al_2O_2Cl_2$	384.2							
Al_2OCl_4	444.9							
Al_2O_3	293.3	298.9					5.6	
Al_2OCl_3	425.1							

All values computed from frequencies obtained after geometry optimisation with specified functional. Final column indicates maximum unsigned error between DFT–DFT and DFT–literature values. [a]with the aug-cc-pVTZ basis set.

Figure 5 is also included, which shows only the very upper part of the concentration plot in order to show the specific species that are most stable. Interestingly, $AlCl_3$ is the most stable aluminium species across the temperature range.

For clarity, the individual species concentrations in Figure 4 have been consolidated into the following groups: Ti oxychlorides ($TiOCl$, $TiOCl_2$, $TiOCl_3$, TiO_2Cl_2, TiO_2Cl_3, $Ti_2O_2Cl_3$, $Ti_2O_2Cl_4$, $Ti_2O_3Cl_2$, $Ti_2O_3Cl_3$, $Ti_3O_4Cl_4$, $Ti_5O_6Cl_8$, $Ti_2O_2Cl_6$, $Ti_2O_2Cl_5$, and $TiCl_2OCl$), Al chlorides (Al_2Cl_6, $AlCl_2$, $AlCl_3$, and $AlCl$), Ti chlorides ($TiCl_4$, $TiCl_3$, $TiCl_2$, and $TiCl$), chlorine oxides (ClO, Cl_2O, and ClO_2), Al monomers (AlO_2Cl_2, $AlOCl_2$, AlO_2Cl, $AlOCl$, $AlOCl_3$, AlO_2, and AlO), Ti-Al species (AlO_3ClTi, AlO_2Cl_2Ti, AlO_2Cl_4Ti, AlO_3Cl_2Ti, AlO_2Cl_3Tia, AlO_2Cl_5Ti, $AlOCl_5Ti$, $AlOCl_4Ti$, AlO_2Cl_3Tib, $AlCl_7Ti$, and $AlCl_6Ti$) and Al dimers ($Al_2O_3Cl_2$, $Al_2O_2Cl_3$, $Al_2O_2Cl_2$, Al_2OCl_4, Al_2OCl_3, Al_2O_2Cl, and Al_2O_3). There are ~ 50 species overall in the system. Oxygen and chlorine gases have been omitted from Figure 4, as their overall concentrations show little variation with temperature. The computed equilibrium compositions at other sensible initial $AlCl_3$ concentrations do not differ considerably with respect to the logarithmic scale, nor did pressure influence the position of equilibrium substantially.

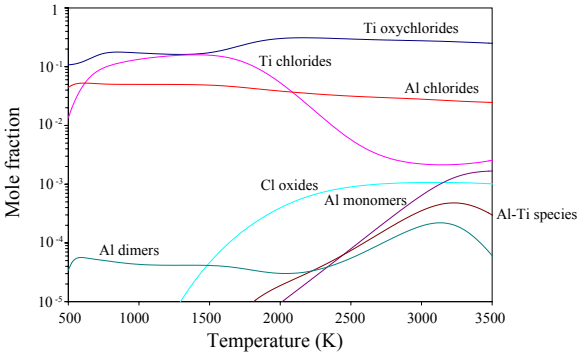

Figure 4: *Computed equilibrium for a* combined *Al/Ti system, initially 5 mol% $AlCl_3$, 47.5 mol% $TiCl_4$ and O_2 at 101.3 kPa. Thermochemical data for Ti species from [31] and the NASA database [20]. For clarity, individual species are grouped, oxygen/chlorine omitted.*

AlO_2Cl_2Ti, AlO_3ClTi, and $AlOCl_4Ti$ are the most populous species containing both titanium and aluminium but none of these is present above a mole fraction of 10^{-5} at temperatures below 2000 K. This suggests that there is little interaction between $AlCl_3$ and $TiCl_4$ in the gas phase. Comparison to the equilibrium plots reported by West *et al.*[30] show that the new aluminium species have little to no effect on the equilibrium curves of the titanium species when $AlCl_3$ is present at the low concentrations used in industry. However, It is still possible that $AlCl_3$ reacts to form Al_2O_3 particles much faster than $TiCl_4$ decomposes and that these Al_2O_3 particles act as nucleation sites. Further investigation in to the gas phase kinetics is required.

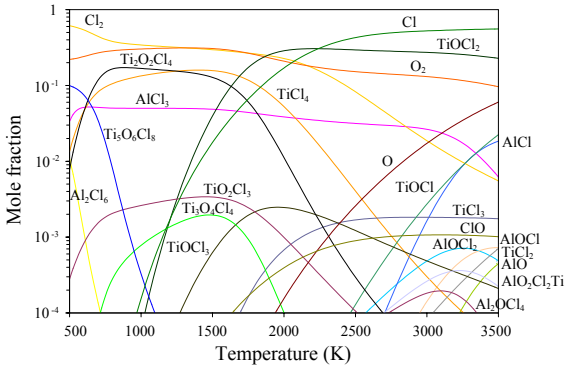

Figure 5: *Computed equilibrium for a* combined *Al/Ti system, initially 5 mol% $AlCl_3$, 47.5 mol% $TiCl_4$ and O_2 at 101.3 kPa. Thermochemical data for Ti species from [31] and the NASA database [20]. Only the very top of the equilibrium plot is shown. The majority of species are excluded.*

4 Conclusion

This work has extended the detailed thermochemistry of the gas-phase titanium oxychloride species investigated by West *et al.*[29] to a similar system of aluminium-containing species. These were not previously included in their work but play an important role in the industrial combustion synthesis of rutile TiO_2. New aluminium species have been proposed through automated species generation and investigated using *ab initio* and DFT methods of computational quantum chemistry. This enabled detailed thermochemical data to be computed for the generated species, many of which have not been reported in the literature and are impossible to obtain with currently available experimental techniques.

Using the thermochemical data, temperature-dependent equilibrium compositions were obtained through simulations at industrially-relevant operating conditions. The aluminium–titanium species are only found to exist at very low concentrations. This seems to suggest that there is not significant interaction between the two systems in the early stages of the reaction. It seems to suggest that $AlCl_3$ is likely to impact the particle processes rather than the gas phase chemical reactions, or that its impact is purely physical. Further studies into the kinetics of the $TiCl_4/AlCl_3/O_2$ system are required in order to make reliable conclusions about the stage at which $AlCl_3$ might determine phase.

5 Acknowledgments

The authors thank Tioxide Europe Limited (TEL) for the financial support of R.A.S. and the EPSRC for help in the form of research hopping grant number EP/E01724X-1.

References

[1] C. Adamo and V. Barone. Exchange functionals with improved long-range behavior and adiabatic connection methods without adjustable parameters: The mPW and mPW1PW models. *J. Chem. Phys.*, 108(2):664–675, 1998. doi:10.1063/1.475428.

[2] M. K. Akhtar, S. E. Pratsinis, and S. V. R. Mastrangelo. Vapor-phase synthesis of Al-doped titania powders. *J. Mater. Res.*, 9:1241–1249, 1994. doi:10.1557/JMR.1994.1241.

[3] A. D. Becke. Density-functional thermochemistry. III. The role of exact exchange. *J. Chem. Phys.*, 98(7):5648–5651, 1993. doi:10.1063/1.464913.

[4] M. W. Chase Jr. NIST-JANAF thermochemical tables, fourth edition. *J. Phys. Chem. Ref. Data*, Monograph 9:I–II, 1998.

[5] C. J. Cramer. *Essentials of Computational Chemistry*. Wiley, 2003.

[6] J. C. Deberry, M. Robinson, M. Pomponi, A. J. Beach, Y. Xiong, and K. Akhtar. Controlled vapor phase oxidation of titanium tetrachloride to manufacture titanium dioxide. US Patent 6,387,347, 2002. URL http://www.google.com/patents?id=r3gKAAAAEBAJ.

[7] S. R. Desai, H. Wu, C. M. Rohlfing, and L.-S. Wang. A study of the structure and bonding of small aluminum oxide clusters by photoelectron spectroscopy: $Al_xO_y^-$ (x = 1–2, y = 1–5). *J. Chem. Phys.*, 106(4):1309–1317, 1997. doi:10.1063/1.474085. URL http://link.aip.org/link/?JCP/106/1309/1.

[8] J. Emsley. *Molecules at an Exhibition*. Oxford University Press, 1999.

[9] M. J. Frisch, G. W. Trucks, H. B. Schlegel, G. E. Scuseria, M. A. Robb, J. R. Cheeseman, J. A. Montgomery, Jr., T. Vreven, K. N. Kudin, J. C. Burant, J. M. Millam, S. S. Iyengar, J. Tomasi, V. Barone, B. Mennucci, M. Cossi, G. Scalmani, N. Rega, G. A. Petersson, H. Nakatsuji, M. Hada, M. Ehara, K. Toyota, R. Fukuda, J. Hasegawa, M. Ishida, T. Nakajima, Y. Honda, O. Kitao, H. Nakai, M. Klene, X. Li, J. E. Knox, H. P. Hratchian, J. B. Cross, V. Bakken, C. Adamo, J. Jaramillo, R. Gomperts, R. E. Stratmann, O. Yazyev, A. J. Austin, R. Cammi, C. Pomelli, J. W. Ochterski, P. Y. Ayala, K. Morokuma, G. A. Voth, P. Salvador, J. J. Dannenberg, V. G. Zakrzewski, S. Dapprich, A. D. Daniels, M. C. Strain, O. Farkas, D. K. Malick, A. D. Rabuck, K. Raghavachari, J. B. Foresman, J. V. Ortiz, Q. Cui, A. G. Baboul, S. Clifford, J. Cioslowski, B. B. Stefanov, G. Liu, A. Liashenko, P. Piskorz, I. Komaromi, R. L. Martin, D. J. Fox, T. Keith, M. A. Al-Laham, C. Y. Peng, A. Nanayakkara, M. Challacombe, P. M. W. Gill, B. Johnson, W. Chen, M. W. Wong, C. Gonzalez, and J. A. Pople. Gaussian 03, Revision C.02, 2003. Gaussian, Inc., Wallingford, CT, 2004.

[10] R. A. Gonzalez, C. D. Musick, and J. N. Tilton. Process for controlling agglomeration in the manufacture of TiO_2. US Patent 5,508,015, April 1996. URL http://www.google.com/patents?id=N80mAAAAEBAJ.

[11] D. G. Goodwin. An open source, extensible software suite for CVD process simulation. In M. Allendorff, F. Maury, and F. Teyssandier, editors, *Chemical Vapor Deposition XVI and EUROCVD 14*, volume 2003-08 of *ECS Proceedings*, pages 155–162, Pennington, New Jersey, USA, 2003. The Electrochemical Society, The Electrochemical Society. URL www.cantera.org.

[12] S. Gordon and B. J. McBride. Computer program for calculation of complex chemical equilibrium composition, rocket performance, incident and reflected shocks and chapman-jouguet detonations. Technical Report NASA-SP-273, NASA, Glenn Research Center, Cleveland, OH, 1976. URL http://hdl.handle.net/2060/19780009781.

[13] F. A. Hamprecht, A. J. Cohen, D. J. Tozer, and N. C. Handy. Development and assessment of new exchange-correlation functionals. *J. Chem. Phys.*, 109(15):6264–6271, October 1998. doi:10.1063/1.477267.

[14] D. L. Hildenbrand, K. H. Lau, and S. V. R. Mastrangelo. Gaseous species in the Ti-Al-Cl system and reaction with H_2O. *J. Phys. Chem.*, 95:3435–3437, 1991. doi:10.1021/j100161a087.

[15] M. M. Islam, T. Bredow, and A. Gerson. Electronic properties of oxygen-deficient and aluminum-doped rutile TiO_2 from first principles. *Phys. Rev. B*, 76:045217, 2007. doi:10.1103/PhysRevB.76.045217.

[16] B. Karlemo, P. Koukkari, and J. Paloniemi. Formation of gaseous intermediates in titanium(IV) chloride plasma oxidation. *Plasma Chem. Plasma Process.*, 16:59–77, 1996. doi:10.1007/BF01465217.

[17] C. T. Lee, W. T. Yang, and R. G. Parr. Development of the colle-salvetti correlation-energy formula into a functional of the electron-density. *Phys. Rev. B*, 37(2):785–789, Jan 1988.

[18] J. E. Lee, S.-M. Oh, and D.-W. Park. Synthesis of nano-sized al doped tio2 powders using thermal plasma. *Thin Solid Films*, 457(1): 230 – 234, 2004. ISSN 0040-6090. doi:DOI: 10.1016/j.tsf.2003.12.027. URL http://www.sciencedirect.com/science/article/B6TW0-4CC1SKS-V/2/d7304c07db8a5ba604b482c2f2be1960. The 16th Symposium on Plasma Science for Materials (SPSM-16).

[19] D. R. Lide, editor. *CRC Handbook of Chemistry and Physics*, volume 5-4: 'Standard thermodynamic properties of chemical substances'. Taylor and Francis, 87th edition, 2007.

[20] B. J. McBride, M. J. Zehe, and S. Gordon. NASA Glenn coefficients for calculating thermodynamic properties of individual species. Technical Report TP-2002-211556, NASA, Glenn Research Center, Cleveland, OH, 2002. URL http://hdl.handle.net/2060/20020085330.

[21] J. P. Perdew. *Elec. Struc. Sol. '91*, page 11. Akademie Verlag, Berlin, 1991.

[22] D. Reidy, J. Holmes, and M. Morris. The critical size mechanism for the anatase to rutile transformation in tio2 and doped-tio2. *J. Europe. Ceram. Soc.*, 26(9):1527 – 1534, 2006. ISSN 0955-2219. doi:DOI: 10.1016/j.jeurceramsoc.2005.03.246. URL http://www.sciencedirect.com/science/article/B6TX0-4G7JXN8-1/2/0778c26b4e06c568a52338bfda6114c4.

[23] P. C. Santos. Production of titanium dioxide. US Patent 3,505,091, April 1970. URL http://www.google.com/patents?id=FiVjAAAAEBAJ.

[24] R. Shirley, O. R. Inderwildi, and M. Kraft. Electronic and optical properties of aluminium-doped anatase and rutile tio_2 from ab initio calculations. c4e-Preprint Series (http://como.cheng.cam.ac.uk) Technical Report 71, c4e-Preprint Series, Cambridge, 2009.

[25] M. Soerlie and H. A. Oeye. Complexation and reduction-oxidation equilibriums of titanium chlorides in gaseous aluminum chloride. *Inorg. Chem.*, 17(9):2473–2484, 1978. doi:10.1021/ic50187a028. URL http://pubs.acs.org/doi/abs/10.1021/ic50187a028.

[26] P. J. Stephens, F. J. Devlin, C. F. Chabalowski, and M. J. Frisch. Ab initio calculation of vibrational absorption and circular dichroism spectra using density functional force fields. *J. Phys. Chem.*, 98(45):11623–11627, 1994.

[27] M. Steveson, T. Bredow, and A. R. Gerson. MSINDO quantum chemical modelling study of the structure of aluminium-doped anatase and rutile titanium dioxide. *Phys. Chem. Chem. Phys.*, 4(2):358–365, 2002. doi:10.1039/b108530c.

[28] Z. Varga and M. Hargittai. Structures and thermodynamic properties of aluminum oxyhalides: a computational study. *Struct. Chem.*, 19(4):595–602, 08 2008. URL http://dx.doi.org/10.1007/s11224-008-9329-4.

[29] R. H. West, G. J. O. Beran, W. H. Green, and M. Kraft. First-principles thermochemistry for the production of TiO_2 from $TiCl_4$. *J. Phys. Chem. A*, 111(18):3560–3565, 2007. doi:10.1021/jp0661950.

[30] R. H. West, M. S. Celnik, O. R. Inderwildi, M. Kraft, G. J. O. Beran, and W. H. Green. Toward a comprehensive model of the synthesis of TiO_2 particles from $TiCl_4$. *Ind. Eng. Chem. Res.*, 46(19):6147–6156, 2007. ISSN 0888-5885. doi:10.1021/ie0706414.

[31] R. H. West, R. A. Shirley, M. Kraft, C. F. Goldsmith, and W. H. Green. A detailed kinetic model for combustion synthesis of titania from $TiCl_4$. *Combust. Flame*, 156: 1764–1770, 2009. doi:10.1016/j.combustflame.2009.04.011.